

# Enzyme-Specific Doxorubicin Drug Beacon as Drug-Resistant Theranostic Molecular Probes

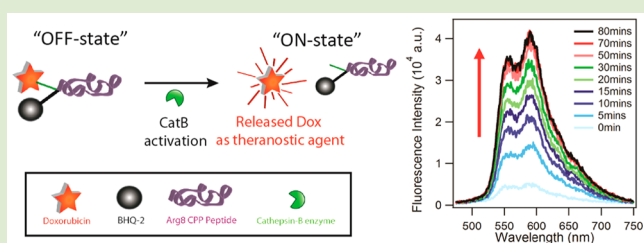
Lye Lin Lock,<sup>†</sup> Zidu Tang,<sup>†</sup> Daniel Keith,<sup>†</sup> Claudia Reyes,<sup>†</sup> and Honggang Cui<sup>\*,†,‡</sup>

<sup>†</sup>Department of Chemical and Biomolecular Engineering, and Institute for NanoBioTechnology, The Johns Hopkins University, 3400 North Charles Street, Baltimore, Maryland 21218, United States

<sup>‡</sup>Department of Oncology and Sidney Kimmel Comprehensive Cancer Center, Johns Hopkins University School of Medicine, Baltimore, Maryland 21205, United States

## S Supporting Information

**ABSTRACT:** We report here on the use of anticancer drug doxorubicin (Dox) to construct a Förster resonance energy transfer (FRET)-based theranostic molecular probe by covalently linking together through a lysine junction a fluorescent drug, a black hole quencher, and a cell-penetrating peptide. We show that upon cleavage by the target lysosomal protease cathepsin B (CatB) the designed drug beacon could release the fluorescent drug serving as an indicator for CatB. Our cell studies suggest that the drug-beacon design can help to circumvent the Dox drug resistance in NCI/ADR-Res ovarian cancer cells, showing significant improvement in cell cytotoxicity compared to the free drug. We believe our design opens up new opportunities to exploit the new functional and structural features of anticancer drugs in addition to their characteristic cytotoxicity.



Proteases are known to play a critical role in the development and progression of many human diseases such as cancer.<sup>1–3</sup> Accordingly, a number of oncological treatments have targeted the overexpression and abnormal activities of cancer-relevant proteases for on-site release of drugs,<sup>4–6</sup> enzyme-responsive diagnostic agents,<sup>7</sup> enzyme-triggered therapy<sup>8</sup> and imaging,<sup>9</sup> as well as the development of protease inhibitor drugs.<sup>10</sup> One particular application has been the creation of polymer–drug and peptide–drug conjugates through an enzymatically activatable linker to improve the tumor targeting efficiency and to circumvent multidrug resistance mechanisms.<sup>4,11–15</sup> In such a prodrug design, the release rate and location of the conjugated drug are primarily determined by the enzymatic activities of the protease of interest. Therefore, in conjunction with the development of novel molecular imaging agents for cancer detection and prognosis, great effort has been devoted to the design of activatable molecular probes for sensing protease activities.<sup>16–21</sup> For example, Chen and co-workers reported the design of protease-activatable probes for matrix metalloproteinase detection.<sup>22</sup> The activation mechanism for these optical probes is primarily based upon a change in Förster resonance energy transfer (FRET) between a pair of fluorescing reporter and quencher moieties before and after the enzymatic degradation. In this communication, we report the design, synthesis, and *in vitro* evaluation of a doxorubicin (Dox) drug-beacon system, which to the best of our knowledge is the first enzyme-specific Dox prodrug conjugated with a dark chromophore quencher, possessing both therapeutic and diagnostic functions. The designed Dox drug beacon was also found to circumvent the

drug-resistant mechanism in NCI/ADR-Res ovarian cancer cells and induce higher cytotoxicity relative to the free Dox.

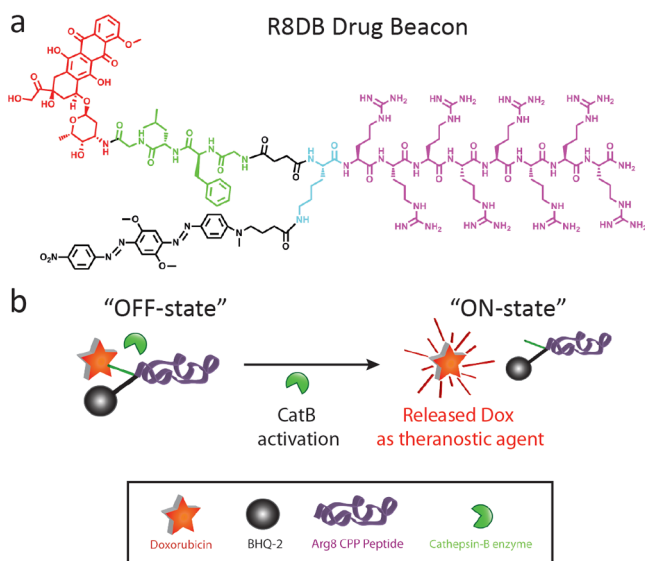
Scheme 1 shows the chemical structure and the expected activation mechanism of the designed Dox drug beacon (R8DB) containing four major components. First, the anticancer drug Dox, the reporter moiety, is an anthracycline antibiotic that has been widely used as a chemotherapeutic drug for various cancer treatments,<sup>23</sup> emitting a red fluorescence in the range of 560–590 nm when excited at 480 nm. Second, Black Hole Quencher-2 (BHQ-2) was chosen as the acceptor/quencher moiety due to its strong and broad absorbance from 500 to 650 nm. Its pairing with Dox is expected to effectively quench the Dox fluorescence through the FRET mechanism due to its absorption overlap with the Dox emission. Upon excitation, BHQ-2 preferentially relaxes to the ground state through nonradiative processes instead of generating new photons, thereby offering a high signal-to-noise ratio. This FRET-based concept has been extensively used to construct molecular beacons for sensing of DNA, RNA, and other biomolecules.<sup>24–27</sup> Third, the tetrapeptide –GFLG–, a well-established cathepsin B (CatB) substrate,<sup>11,28</sup> was used as the cleavable linker to bridge the drug to the BHQ-2 quencher through a lysine junction, modulating the release of Dox while serving as a CatB sensor. Cathepsin B is a lysosomal protease known to be overexpressed in many types of cancer.<sup>29–34</sup> Finally, octa-arginine (R8), a well-studied cell penetrating

Received: March 8, 2015

Accepted: April 24, 2015

Published: April 29, 2015

**Scheme 1. (a) Chemical Structure of the Designed R8DB Drug Beacon with Octa-Arginine Sequence (Purple), –GFLG-Linker (Green), Dox (Red), and BHQ-2 (Black) and (b) Schematic Illustration of R8DB Activation from the OFF-State to ON-State After Cathepsin B Degradation<sup>a</sup>**



<sup>a</sup>The designed Dox drug beacon is expected to remain dark (OFF-state) prior to cellular entry. Following cellular uptake and CatB cleavage of the –GFLG-linker, Dox will be released thus emitting fluorescence while acting as a therapeutic agent (ON-state).

peptide (CPP) sequence,<sup>35</sup> was used to assist in the effective cellular internalization.<sup>36</sup> All the molecules studied here were synthesized using a combined automatic and manual solid-phase peptide synthesis (SPPS) method as reported previously.<sup>19</sup> After HPLC purification, analytical HPLC and mass spectrometry were used to confirm the purity and expected molecular mass for the synthesized compounds. Their details can be found in the Supporting Information (SI, Schemes S1–S3).

We first determined the quenching efficiency of BHQ-2 after its conjugation onto the Dox beacon. In this fluorescence experiment, we excited the R8DB solution (3  $\mu$ M in 1 $\times$ PBS) at 465 nm and collected the emission spectra as shown in Figure 1a, with the free Dox of the same molar concentration as the control. The quenching efficiency was calculated to be  $90.6 \pm 1.6\%$ , equivalent to a 10-fold decrease in Dox fluorescence intensity after incorporating the BHQ-2 quencher. Next, in an effort to demonstrate the enzyme-responsive feature of the R8DB drug beacon and its possible use for CatB sensing, we studied their activation in a CatB-containing solution and measured their emission spectra at different time points. The fluorescence intensity of a 3  $\mu$ M R8DB drug beacon aqueous solution was observed to increase gradually after exposure to 0.05 Units (U) of CatB enzyme for 80 min, exhibiting the typical emission spectrum of free Dox (Figure 1b). According to the work by Kopecek and co-workers,<sup>28</sup> CatB was reported to cleave the GFLG linker at the amide bond of F and L, as well as at the C-terminal of GFLG. Therefore, two residues could still be possibly attached to Dox (Dox-GL) upon initial cleavage which could undergo further degradation to release free Dox over time.<sup>37</sup> To evaluate the Dox release profiles, we monitored the change in Dox fluorescence intensity over time in the presence of varying concentrations of CatB (Figure 1c). We

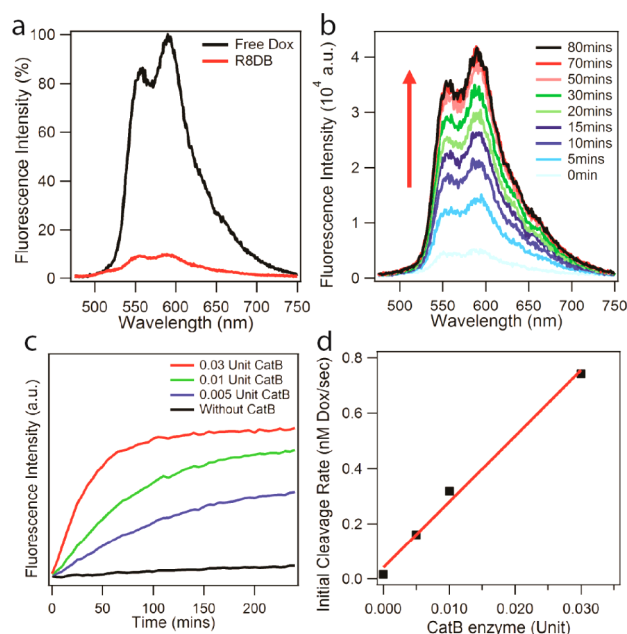


**Figure 1.** (a) Fluorescence emission spectra of free Dox (black line) and R8DB (red line) at 3  $\mu$ M. (b) Fluorescence emission spectra of a 3  $\mu$ M R8DB solution at different time points after introducing 0.05 U of CatB. (c) Changes in fluorescence intensity of a 3  $\mu$ M R8DB solution in the presence of various amounts of CatB: 0.00 U (black), 0.005 U (blue), 0.01 U (green), and 0.03 U (red). (d) Plot of initial cleavage rates (obtained from time 0–30 min of (c)) shows a linear correlation with the CatB concentration.

observed that the R8DB solution without CatB showed a minimum level of Dox fluorescence throughout the course of the study (OFF-state), while solutions containing 0.005 U, 0.01 U, and 0.03 U of CatB exhibited a rapid increase in Dox fluorescence (ON-state), commensurate with the amount of CatB used. The initial cleavage rates were obtained from the slope between  $t = 0$  and  $t = 30$  min and found to scale linearly with the CatB concentration (Figure 1d). The  $k_{\text{cat}}/K_M$  value was calculated to be  $568.4 \text{ (mol/L)}^{-1}\cdot\text{s}^{-1}$  using the simplified Michaelis–Menten equation (S2 in SI). This number is four times as high as our previous finding in a different molecular beacon system<sup>19</sup> and is in the same order of magnitude with other systems using the same peptide substrate.<sup>11</sup> This implies that the drug-beacon design does not compromise the cleavage specificity of the GFLG substrate by CatB. These results also clearly suggest that the R8DB drug beacon can be specifically activated by the CatB enzyme, recovering the drug's native fluorescence for intracellular tracking and/or CatB sensing.

We further evaluated the theranostic feature of the R8DB drug beacon in a drug-resistant ovarian cancer cell line. It is well-known that Dox is transported into cells through a passive diffusion mechanism and subsequently accumulates in the cell nucleus whereupon intercalation with DNA occurs to induce cell apoptosis. However, drug-resistant cell lines could have evolved with a defensive system known as P-glycoprotein efflux pump to avoid accumulation of drug above its cytotoxic threshold.<sup>38</sup> For a better comparison of drug internalization and efficacy, we incubated 3  $\mu$ M Dox and R8DB drug beacon, respectively, in the drug-resistant NCI/ADR-Res ovarian cancer cells, followed by fluorescence imaging of live cells using confocal laser scanning microscopy (Figure 2). Cells after 72 h of incubation were replaced with fresh media containing either

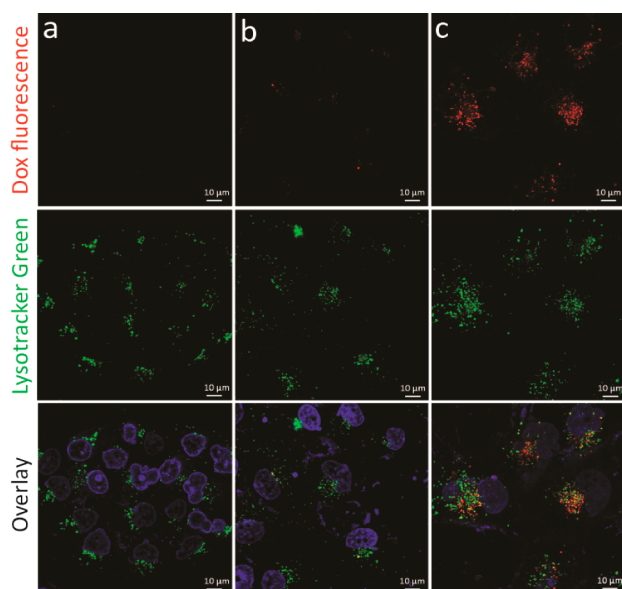


**Figure 2.** Live cell confocal images of NCI/ADR-Res drug-resistant ovarian cancer (a) without any drug (blank), (b) in the presence of 3  $\mu\text{M}$  free Dox, and (c) in the presence of 3  $\mu\text{M}$  R8DB incubated for 96 h. Dox fluoresced in red, and lysosomal compartments were stained with LysoTracker Green and cell nuclei in blue with Hoechst 33342.

the drug or R8DB drug beacon due to the depletion of nutrition. As shown in Figure 2, it is evident that the R8DB drug beacon (Figure 2c) exhibits much stronger red fluorescence in cells than the free Dox (Figure 2b), indicating both effective cellular internalization and CatB activation. This phenomenon has also been observed in other prodrug designs possessing CPP features that interact with drug-resistant cell lines.<sup>39–41</sup> A few studies have showed that the azo moiety in the BHQ quencher is susceptible to reduction reaction which could possibly give rise to false fluorescence increase.<sup>42,43</sup> However, we have previously shown that under similar experimental conditions BHQ was able to quench and maintained fluorescence of our designed molecular beacon in the presence of CatB inhibitor which is known to suppress CatB's activity in cleaving the GFLG substrate.<sup>19</sup> To validate the subcellular colocalization of the R8DB drug beacon, we selectively stained the lysosomal compartments with LysoTracker Green. As shown in Figure 2c, the red fluorescence coming from the released Dox was mostly located within the lysosomal compartments as they colocalized with LysoTracker Green. This observation confirms our assumption that R8DB drug beacons are internalized by cancer cells through endocytosis pathways.<sup>44–47</sup>

In addition, we have attempted to trace the intracellular Dox localization for longer periods of time; however, cell conditions were severely deteriorated (cells started to die), preventing more detailed analysis of the intracellular trafficking pathways of the Dox beacon. In Figure 2b, the negligible red fluorescence suggests that free Dox entering cells through diffusion is likely pumped out by the cell drug resistance mechanism.<sup>48,49</sup> Therefore, the enhanced accumulation of released Dox in drug-resistant cancer cells means that the R8DB drug beacon could possibly help circumvent the drug-resistance mechanism that many cancer cells could develop over the course of chemotherapy. It should be noted that although the R8DB drug beacon has amphiphilic character and thus the potential to assemble into micellar structures in aqueous solutions, the extremely low concentrations in all experimental conditions (3

$\mu\text{M}$ ) and the prolonged incubation (in days) suggest that R8DB would have most likely remained in its monomeric form in these studies.

To validate the *in vitro* efficacy of the Dox drug-beacon design, a dose–response study was conducted using an SRB assay (Figure 3), using free Dox as control. As expected, free

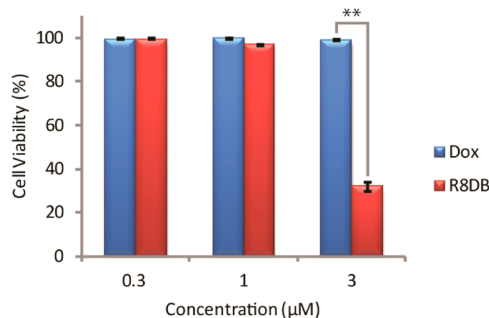


**Figure 3.** Cytotoxicity assay of NCI/ADR-Res cells incubated with various concentrations of free Dox and R8DB drug beacon (0.3–3  $\mu\text{M}$ ). Data are given as mean  $\pm$  sd ( $n = 3$ ). Fresh cell media with respective drugs were used to replace the cell media after 3 days, and the cells were further incubated for another 3 days.  $**P < 0.001$ .

Dox did not exhibit any toxicity after 6 days of incubation for any of the studied concentrations (0.3–3  $\mu\text{M}$ , blue bars in Figure 3). At lower concentrations (0.3 and 1  $\mu\text{M}$ ), the R8DB drug beacon also showed a negligible effect on cell viability (red bars in Figure 3). Although the octa-arginine peptide was known to facilitate the effective internalization of R8DB, the released Dox within the cell could still be lower than the toxicity concentration threshold. At 3  $\mu\text{M}$ , the R8DB drug beacon exhibited remarkable improvement in drug efficacy with only  $\sim 30\%$  of cells remaining viable. This observation is consistent with our confocal imaging study, where R8DB showed higher Dox fluorescence intensity in cells compared to free Dox of the same concentration. Since octa-arginine is a highly positively charged peptide, it could potentially disrupt cell membranes thus causing cytotoxicity.<sup>50</sup> As a result, R8DB concentration was deliberately set below 5  $\mu\text{M}$ , a condition where the R8 peptide sequence was known to show negligible cytotoxicity.<sup>51</sup> Therefore, our cytotoxicity result reflects the drug beacon's ability to overcome the drug-resistance mechanism in NCI/ADR-Res ovarian cancer cells.

In summary, we have reported a novel design of an enzyme-specific theranostic probe by taking advantage of the fluorescence capacity of the anticancer drug Dox. Incorporating a fluorescing drug into the beacon design opens up a new platform to explore the diagnostic functionality of therapeutic agents. This synergistic effect could potentially reduce the discrepancy between tumor diagnostic locations with actual drug-delivered sites, which is one of the important challenges in the current treatment paradigm.

## ■ ASSOCIATED CONTENT

### 📄 Supporting Information

Synthesis and characterization of the R8DB drug beacon, CatB enzymatic activation, confocal laser scanning microscopy, and cell cytotoxicity assay procedures. The Supporting Information is available free of charge on the ACS Publications website at DOI: 10.1021/acsmacrolett.5b00170.

## ■ AUTHOR INFORMATION

## Corresponding Author

\*E-mail: hcui6@jhu.edu.

## Notes

The authors declare no competing financial interest.

## ■ ACKNOWLEDGMENTS

We thank National Science Foundation (DMR 1255281) and the W.W. Smith Charitable Trust for support of the project. We thank the JHU Integrated Imaging Center (IIC) for the use of confocal imaging facility and the JHU Department of Chemistry Mass Spectrometry facility for mass spectrometry analysis.

## ■ REFERENCES

- (1) Duffy, M. J. *Clin. Exp. Metastasis* **1992**, *10*, 145–155.
- (2) Joyce, J. A.; Baruch, A.; Chehade, K.; Meyer-Morse, N.; Giraud, E.; Tsai, F. Y.; Greenbaum, D. C.; Hager, J. H.; Bogyo, M.; Hanahan, D. *Cancer Cell* **2004**, *5*, 443–453.
- (3) Lopez-Otin, C.; Bond, J. S. *J. Biol. Chem.* **2008**, *283*, 30433–30437.
- (4) Chen, Z. P.; Zhang, P. C.; Cheetham, A. G.; Moon, J. H.; Moxley, J. W.; Lin, Y. A.; Cui, H. G. *J. Controlled Release* **2014**, *191*, 123–130.
- (5) Choi, K. Y.; Swierczewska, M.; Lee, S.; Chen, X. *Theranostics* **2012**, *2*, 156–178.
- (6) Pearce, T. R.; Shroff, K.; Kokkoli, E. *Adv. Mater.* **2012**, *24*, 3803–3822.
- (7) Weissleder, R.; Tung, C. H.; Mahmood, U.; Bogdanov, A., Jr. *Nat. Biotechnol.* **1999**, *17*, 375–378.
- (8) Zheng, G.; Chen, J.; Stefflova, K.; Jarvi, M.; Li, H.; Wilson, B. C. *Proc. Nat. Acad. Sci. U.S.A.* **2007**, *104*, 8989–8994.
- (9) Gao, Y.; Shi, J. F.; Yuan, D.; Xu, B. *Nat. Commun.* **2012**, *3*, 1033.
- (10) Adams, J. *Cancer Cell* **2004**, *5*, 417–421.
- (11) Duncan, R.; Cable, H. C.; Lloyd, J. B.; Rejmanova, P.; Kopecek, J. *Macromol. Chem. Phys.* **1983**, *184*, 1997–2008.
- (12) Lin, Y. A.; Cheetham, A. G.; Zhang, P. C.; Ou, Y. C.; Li, Y. G.; Liu, G. S.; Hermida-Merino, D.; Hamley, I. W.; Cui, H. G. *ACS Nano* **2014**, *8*, 12690–12700.
- (13) Tang, L.; Yang, X.; Yin, Q.; Cai, K.; Wang, H.; Chaudhury, I.; Yao, C.; Zhou, Q.; Kwon, M.; Hartman, J. A.; Dobrucki, I. T.; Dobrucki, L. W.; Borst, L. B.; Lezmig, S.; Helfferich, W. G.; Ferguson, A. L.; Fan, T. M.; Cheng, J. *Proc. Nat. Acad. Sci. U.S.A.* **2014**, *111*, 15344–15349.
- (14) Tong, R.; Cheng, J. *Angew. Chem., Int. Ed.* **2008**, *47*, 4830–4834.
- (15) Tong, R.; Tang, L.; Ma, L.; Tu, C. L.; Baumgartner, R.; Cheng, J. *J. Chem. Soc. Rev.* **2014**, *43*, 6982–7012.
- (16) Bremer, C.; Tung, C. H.; Weissleder, R. *Nat. Med.* **2001**, *7*, 743–748.
- (17) Drake, C. R.; Miller, D. C.; Jones, E. F. *Curr. Org. Synth.* **2011**, *8*, 498–520.
- (18) Lee, S.; Xie, J.; Chen, X. Y. *Curr. Top. Med. Chem.* **2010**, *10*, 1135–1144.
- (19) Lock, L. L.; Cheetham, A. G.; Zhang, P. C.; Cui, H. G. *ACS Nano* **2013**, *7*, 4924–4932.
- (20) Razgulin, A.; Ma, N.; Rao, J. H. *Chem. Soc. Rev.* **2011**, *40*, 4186–4216.
- (21) Zhang, P.; Cheetham, A. G.; Lock, L. L.; Li, Y.; Cui, H. *Curr. Opin. Biotechnol.* **2015**, *34C*, 171–179.
- (22) Zhu, L.; Ma, Y.; Kiesewetter, D. O.; Wang, Y.; Lang, L. X.; Lee, S.; Niu, G.; Chen, X. Y. *ACS Chem. Biol.* **2014**, *9*, 510–516.
- (23) Nitiss, J. L. *Nat. Rev. Cancer* **2009**, *9*, 338–350.
- (24) Liu, T. W. B.; Chen, J.; Zheng, G. *Amino Acids* **2011**, *41*, 1123–1134.
- (25) Qiu, L. P.; Wu, C. C.; You, M. X.; Han, D.; Chen, T.; Zhu, G. Z.; Jiang, J. H.; Yu, R. Q.; Tan, W. H. *J. Am. Chem. Soc.* **2013**, *135*, 12952–12955.
- (26) Santra, S.; Kaittanis, C.; Santiesteban, O. J.; Perez, J. M. *J. Am. Chem. Soc.* **2011**, *133*, 16680–16688.
- (27) Wang, H.; Yang, R. H.; Yang, L.; Tan, W. H. *ACS Nano* **2009**, *3*, 2451–2460.
- (28) Rejmanova, P.; Kopecek, J.; Pohl, J.; Baudys, M.; Kostka, V. *Macromol. Chem. Phys.* **1983**, *184*, 2009–2020.
- (29) Gondi, C. S.; Rao, J. S. *Expert Opin. Ther. Targets* **2013**, *17*, 281–291.
- (30) Hwang, J. H.; Lee, K. H.; Lee, K. Y.; Ryu, J. K.; Kim, Y. T.; Yoon, Y. B.; Lee, H. S. *J. Gastroenterol. Hepatol.* **2006**, *21*, A429–A429.
- (31) Krepela, E.; Vicar, J.; Cernoch, M. *Neoplasma* **1989**, *36*, 41–52.
- (32) Li, C. S.; Chen, L. W.; Wang, J. L.; Zhang, L. Y.; Tang, P. Z.; Zhai, S. Q.; Guo, W. W.; Yu, N.; Zhao, L. D.; Liu, M. B.; Yang, S. M. *Oncol. Rep.* **2011**, *26*, 869–875.
- (33) Miyake, H.; Hara, I.; Eto, H. *Anticancer Res.* **2004**, *24*, 2573–2577.
- (34) Wu, D.; Wang, H. J.; Li, Z. N.; Wang, L. H.; Zheng, F. Y.; Jiang, J.; Gao, Y. T.; Zhong, H. F.; Huang, Y.; Suo, Z. H. *Histol. Histopathol.* **2012**, *27*, 79–87.
- (35) Fonseca, S. B.; Pereira, M. P.; Kelley, S. O. *Adv. Drug Delivery Rev.* **2009**, *61*, 953–964.
- (36) Zhang, K.; Fang, H.; Chen, Z.; Taylor, J.-S. A.; Wooley, K. L. *Bioconjugate Chem.* **2008**, *19*, 1880–1887.
- (37) Kurtoglu, Y. E.; Mishra, M. K.; Kannan, S.; Kannan, R. M. *Int. J. Pharmaceut.* **2010**, *384*, 189–194.
- (38) Eckford, P. D.; Sharom, F. J. *Chem. Rev.* **2009**, *109*, 2989–3011.
- (39) Aroui, S.; Brahim, S.; De Waard, M.; Kenani, A. *Biochem. Biophys. Res. Commun.* **2010**, *391*, 419–425.
- (40) Dubikovskaya, E. A.; Thorne, S. H.; Pillow, T. H.; Contag, C. H.; Wender, P. A. *Proc. Nat. Acad. Sci. U.S.A.* **2008**, *105*, 12128–12133.
- (41) Lindgren, M.; Rosenthal-Aizman, K.; Saar, K.; Eiriksdottir, E.; Jiang, Y.; Sassian, M.; Ostlund, P.; Hallbrink, M.; Langel, U. *Biochem. Pharmacol.* **2006**, *71*, 416–425.
- (42) Leriche, G.; Budin, G.; Darwich, Z.; Weltin, D.; Mely, Y.; Klymchenko, A. S.; Wagner, A. *Chem. Commun.* **2012**, *48*, 3224–3226.
- (43) Linder, K. E.; Metcalfe, E.; Nanjappan, P.; Arunachalam, T.; Ramos, K.; Skedzielewski, T. M.; Marinelli, E. R.; Tweedle, M. F.; Nunn, A. D.; Swenson, R. E. *Bioconjugate Chem.* **2011**, *22*, 1287–1297.
- (44) Futaki, S.; Nakase, I.; Taclokoru, A.; Takeuchi, T.; Jones, A. T. *Biochem. Soc. Trans.* **2007**, *35*, 784–787.
- (45) Nakase, I.; Niwa, M.; Takeuchi, T.; Sonomura, K.; Kawabata, N.; Koike, Y.; Takehashi, M.; Tanaka, S.; Ueda, K.; Simpson, J. C.; Jones, A. T.; Sugiura, Y.; Futaki, S. *Mol. Ther.* **2004**, *10*, 1011–1022.
- (46) Zhang, P. C.; Cheetham, A. G.; Lock, L. L.; Cui, H. G. *Bioconjugate Chem.* **2013**, *24*, 604–613.
- (47) Zhang, P. C.; Lock, L. L.; Cheetham, A. G.; Cui, H. G. *Mol. Pharmaceut.* **2014**, *11*, 964–973.
- (48) Fojo, A. T.; Ueda, K.; Slamon, D. J.; Poplack, D. G.; Gottesman, M. M.; Pastan, I. *Proc. Nat. Acad. Sci. U.S.A.* **1987**, *84*, 265–269.
- (49) Gottesman, M. M.; Fojo, T.; Bates, S. E. *Nat. Rev. Cancer* **2002**, *2*, 48–58.
- (50) Schmidt, N.; Mishra, A.; Lai, G. H.; Wong, G. C. L. *FEBS Lett.* **2010**, *584*, 1806–1813.
- (51) Lin, R.; Zhang, P.; Cheetham, A. G.; Walston, J.; Abadir, P.; Cui, H. *Bioconjugate Chem.* **2015**, *26*, 71–77.